Subsurface imaging of brown coal bearing Tertiary sedimentaries - Deccan Trap interface using microtremor method

Dhananjay A. Sant [a,*], Imtiyaz A. Parvez [b], Govindan Rangarajan [c], Satish J. Patel [a], T.A. Sanoop Salam [a], Madhuri N. Bhatt [a]

[a] Department of Geology, Faculty of Science, The Maharaja Sayajirao University of Baroda, Vadodara 390002. India
[b] CSIR Fourth Paradigm Institute (Formerly CSIR Centre for Mathematical Modeling and Computer Simulation; C-MMACS), NAL Belur Campus, Bengaluru 560 037, India
[c] Department of Mathematics, Indian Institute of Science, Bangalore, Bengaluru 560 012, India

ARTICLE INFO

ABSTRACT

We propose an application of the microtremor (ambient noise) H/V spectral ratio technique to identify significant rheological boundaries at shallow depths, estimate thickness of both lignite bearing Tertiary sedimentary sequence and late Cretaceous Deccan basalt flows and comprehend basinal geometry of Umarsar Basin (Babia syncline). Forty-six stations were gauged in a grid format at ~250 m resolution during the microtremor survey. The microtremor H/V spectral ratio technique takes into account the frequency of the ratio between the horizontal (NS + EW) and vertical components of persistent Rayleigh waves in the area. Depth estimates are made using Mean_Vs (433.69 m/s) from three borehole records (MMA_Vs (431.6 m/s), MMB_Vs (406.86 m/s) and MMC_Vs (462.6 m/s) using standard relationship between depth and velocity. In the present study, we recognize three rheological interfaces viz., L_1 interface (0.2328 Hz to 0.3862 Hz), L_2 interface (0.7843 Hz to 2.5123 Hz) and L_3 interface (6.2477 Hz to 27.1119 Hz). The geology and stratigraphic records supplement correlation for L_1, L_2 and L_3 interfaces with Mesozoic–Deccan Trap (M-DT) boundary, Deccan Trap-Tertiary (DT-T) boundary, and boundaries between shale carbonate hardpans within sediment sequence belonging to Naredi Formation respectively. The estimated depth range for M-DT boundary (L_1) is 281–466 m and for DT-T boundary (L_2) is 43–138 m. The subsurface image acquired from the frequency records advocates for a palaeo high in SE portion that retains its entity over the present landscape. The frequency records advocate for 369 m to 206 m thick Deccan basalt and 85 m to 18 m thick lignite bearing Naredi Formation. The ambient noise seismic study further suggests NW-SE trending basin geometry of Babia syncline comprising three distinct depressions having six local depocenters. Finally, we propose the microtremor H/V spectral ratio technique as a tool to develop economical borehole plan with realistic reserve estimate and a step forward towards rapid economical assessment covering large mining lease areas complementary to local geological studies.

© 2018 Elsevier B.V. All rights reserved.

1. Introduction

The Indian Tertiary brown coals (lignite) that are commercially mined in states of Gujarat, Rajasthan, Jammu & Kashmir, Kerala, Tamil Nadu and Pondicherry (Mineral Reviews Part-III, 2017) can be placed together in a regional context (Sanfilipo et al., 1992; Kumar et al., 2014). The synchronous Tertiary brown coal development occurs within widely spaced basins in Indian subcontinent as well as across globe viz., Europe, Africa, South America, North American and Australia are further envisaged to be governed through eustatically driven mechanism instead of localized structural control (World Energy Council, 2013). In the state of Gujarat, reserves of brown coal are reported from Panandhro, Matanomadh, Umarsar (western Kachchh Basin: Biswas, 1992: Fig. 1); Bhavnagar (western fringe of Cambay Basin: Thakur et al., 2010); and Rajpardi-Vastan (eastern fringe of Cambay Basin: Chandra and Chowdhary, 1969 and Agrawal, 1984; Sahni et al., 2006); Mahesana - Kalol subsurface lignite (north Cambay Basin: Das et al., 2006). The potential of brown coal are further proved across Great Rann of Kutch into Rajasthan (Barmer and Bikaner: Kumar et al., 2014) and in Sindh province of Pakistan (Sanfilipo et al., 1992). Drilling boreholes in a gridded array up to certain fixed depth has remained a popular method to carry out exploration for brown coal in the region as well as in the lease areas. We propose the microtremor H/V spectral ratio technique as a geophysical tool for the first time to explore the same. The microtremor measurements supplemented with few exploratory boreholes provide an understanding of basin morphology (shallow, deep or marginal portion within

* Corresponding author.
E-mail addresses: sant.dhananjay-geology@msubaroda.ac.in (D.A. Sant), parvez@csir4pi.in (I.A. Parvez), rangaraj@math.iisc.ernet.in (G. Rangarajan), patel.satish-geology@msubaroda.ac.in (S.J. Patel).
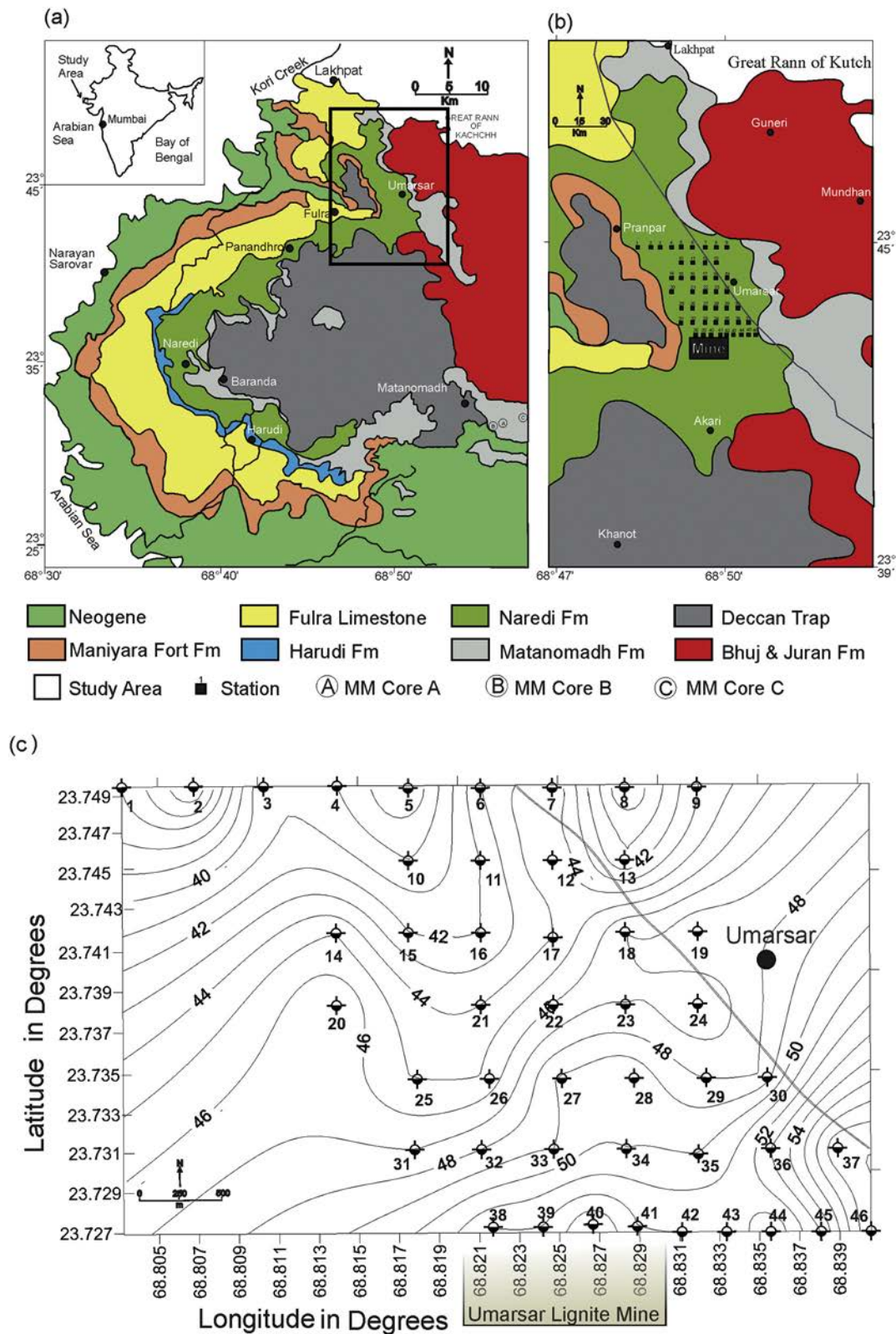
Fig. 1. (a)Regional geological map of NW Kachchh Mainland (after Biswas, 1992 and Saraswati et al., 2016). MM Core A, MM Core B, and MM Core C are located SE of Matanomadh village. (b)Geological map of the study area. (c)Half filled circle in a grid format are the sites of microtremor measurement (stations 1 to 46) placed along with topographic contours at Umarsar lease area.

basin). The results obtained from such studies would assist mine planner to decide boreholes location, their depths and number of boreholes reducing cost of exploration and leads to better reserves estimation.

In the present study, we exemplify results from our microtremor survey (during field season December 2014) in upcoming lease area of Umarsar lignite mine in western Kachchh. In the study area the lignite bearing lower Tertiary sedimentary sequence imparts a strong

impedance contrast with underlying Deccan Traps (basalt flows) giving a strong H/V resonant frequency peak that can draw a parallel with depth of Deccan Trap-Tertiary sedimentary interface. The microtremor measurements supplemented with geology have enabled us *(i)* to map pre-Tertiary highs and lows, *(ii)* to estimate thickness of lignite bearing sedimentary sequence (Neardi Formation) and underneath Deccan basalt, *(iii)* to develop subsurface image for Mesozoic–Deccan Trap and Deccan Trap-Tertiary boundaries and *(iv)* to decode architecture of Umarsar basin (Babia syncline).

2. Geology

In the western Kachchh, brown coal is well developed within the early Tertiary (Eocene-Paleocene) sedimentary sequence (Naredi Formation/Matanomadh Formation) aggraded over late Cretaceous Deccan Traps and Mesozoic sedimentary sequence (Fig. 1, Table 1: Biswas, 1992, 2016; Dutta et al., 2011). The study area forms a part of depression called Babia syncline (Biswas, 1992) bounded by high ground to east exposing Cretaceous sandstone-shale belonging to Bhuj Formation followed by shale-volcanoclastic sequence along western fringe belonging to Matanomadh Formation. The western high ground exposes basalts belonging to late Cretaceous Deccan Traps followed by clay-limestone sequence along eastern fringe belonging to Maniyara Fort Formation (Fig. 1). The study area shows aggradation of thick shale-clay sequence (Naredi Formation) intercalated with lignite and bands and carbonate hardpans of wackestone and packstones (foraminiferal limestone and carbonate rocks; Table 1). that pinch out laterally within shale-clayey Naredi Formation. The sediment sequence was deposited in pre-Tertiary depression in lagoonal to coastal marsh to back swamp environments. Largely the attitude of the Tertiary sediment sequence is horizontal to gentle westerly dip at places (Khozyem et al., 2013).

The shale and volcanoclastic sediment intercalated with lignite seams belonging to Matanomadh Formation (late Paleocene) are exposed further SE of study area. Matanomadh Formation encompasses a shale-dominated sedimentary sequence intermingled with volcanoclastic sediment. The sequence is intercalated with lignite seams at the basal portion whereas calcareous mudstone bands caps the sequence (Dutta et al., 2011). Three exploratory boreholes drilled by Gujarat Mineral Development Cooperation viz., MM Core A(97.5 m deep from the surface), MM Core B(89.5 m deep from the surface) and MM Core C(95 m deep from the surface) SE of Matanomadh village were used to validate the results. The boreholes MM Cores A, B, and C represents a shale-dominated sequence intercalated with 8 to 10 lignite seams (~1 m thickness) followed by Deccan basalt at depth of 96.53 m, 86.5 m, and 93.5 m respectively (Fig. 2).

Table 1
Lithostratigraphy of NW Kachchh Mainland (after Biswas, 1992, 2016).

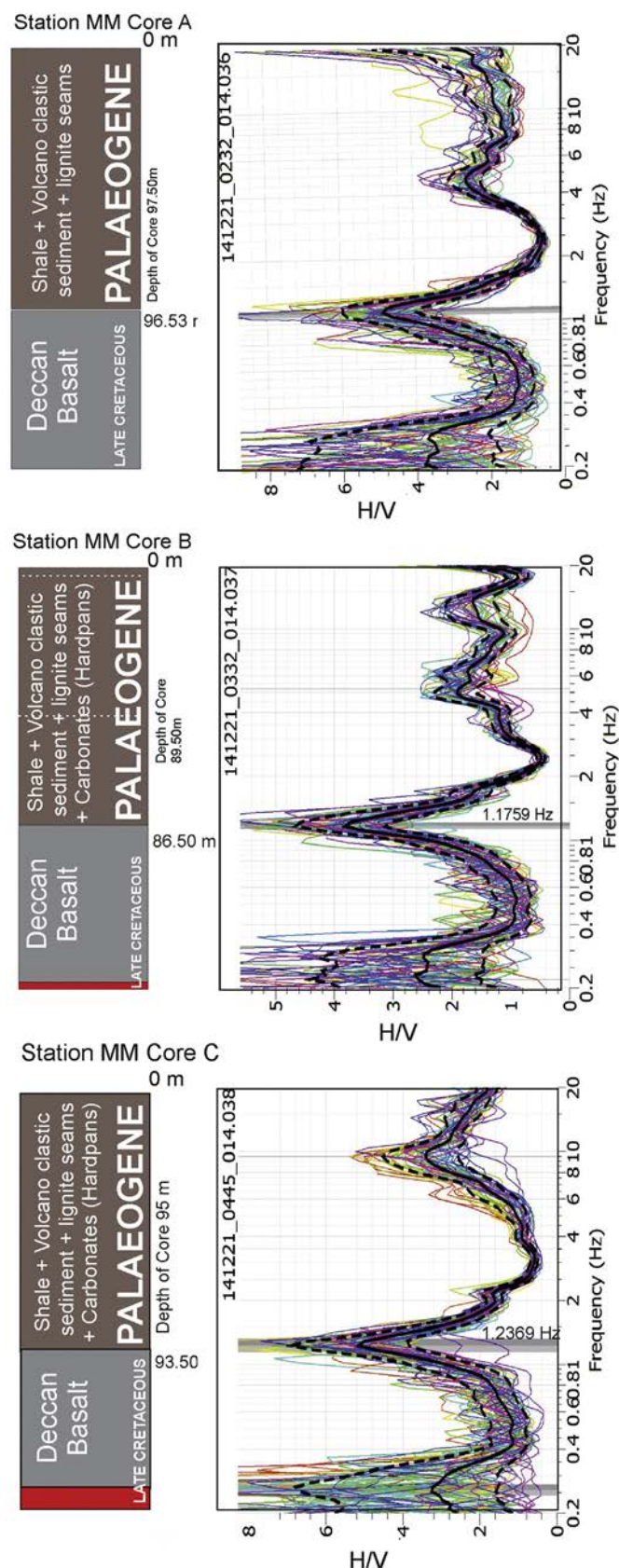| Age	Formation	Lithology
Neogene		
Oligocene	Maniyara fort	Claystone, limestone, glauconitic gypseous shale
Middle Eocene	Fulra limestone	Foraminiferal grainstone and packstone
	Harudi	Claystone, limestone, coquina
Upper Paleocene to Lower Eocene	Naredi	Ferruginous claystone Assilina packstone & wackestone glauconitic gypseous shale
Upper Paleocene	Matanomadh	Laterite, volcanoclastics tuffaceous shales, sandstone, bentonitic clays
Upper Cretaceous	Deccan traps	Basalt
Lower Cretaceous	Bhuj formation	Sandstone, Shale
Upper Jurassic	Juran formation	Calcareous Sandstone, Shale

Fig. 2. Comparison between resonant frequency and the depth of stratigraphic boundary along MM Core A, MM Core B, and MM Core C drilled by Gujarat mineral development corporation SE of Matanomadh village (Fig.1). The resonant frequency 1.1178 Hz (MM Core A), 1.1759 (MM Core B)and 1.2369 (MM Core C)are compared with DT-T boundary along cores at depth 96.53 m, 86.50 m and 93.50 m respectively.
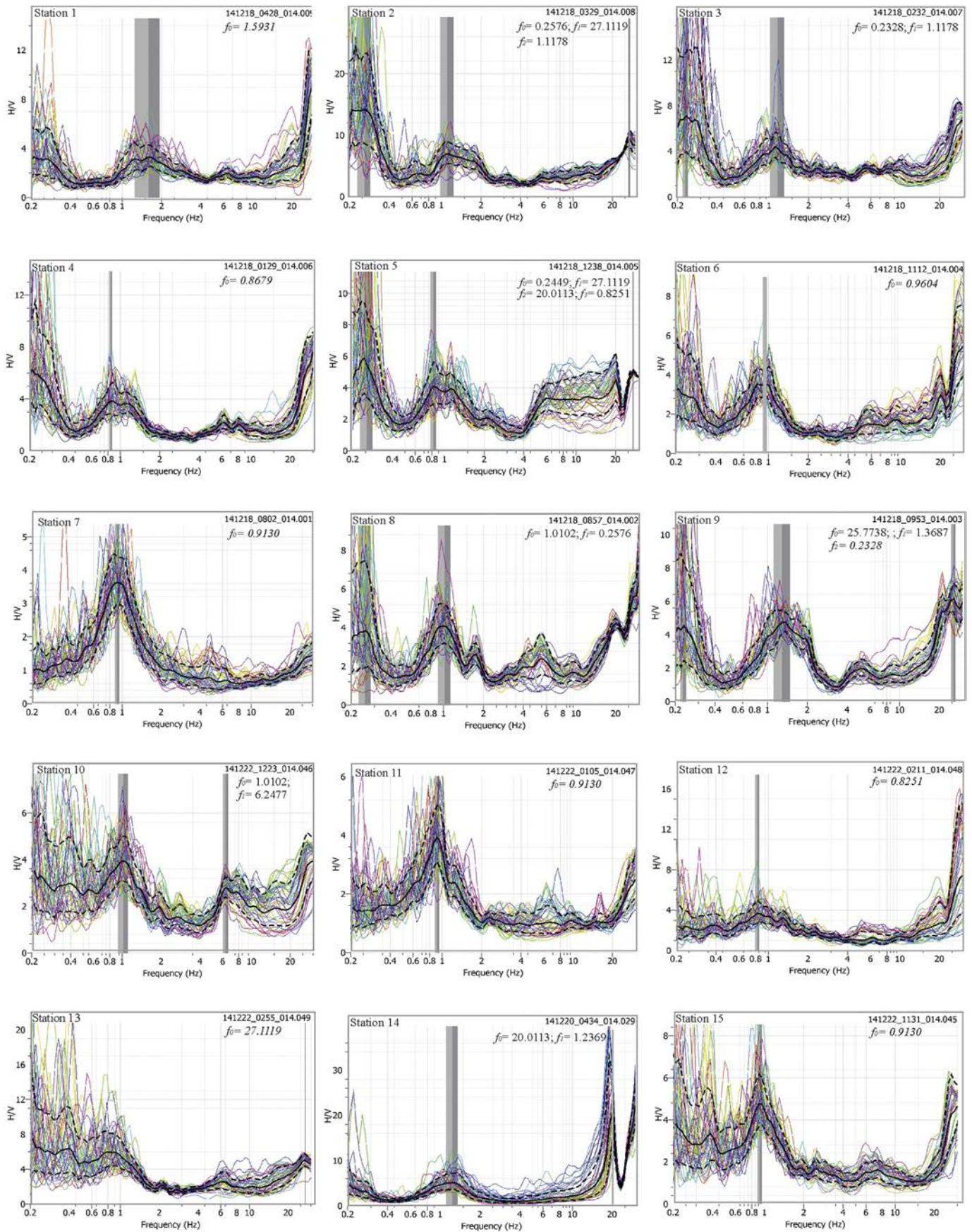
Fig. 3. Scatter plot showing spectral frequency of H/V recorded along stations 1 to 46. The continuous line represents the Mean value of resonant frequency where as dashed line marks mean resonant frequency ± standard deviation. The figures on the right hand side top indicate file number. f_0, f_1, f_2 and f_3 are the resonant frequency peaks at one-sigma significance.
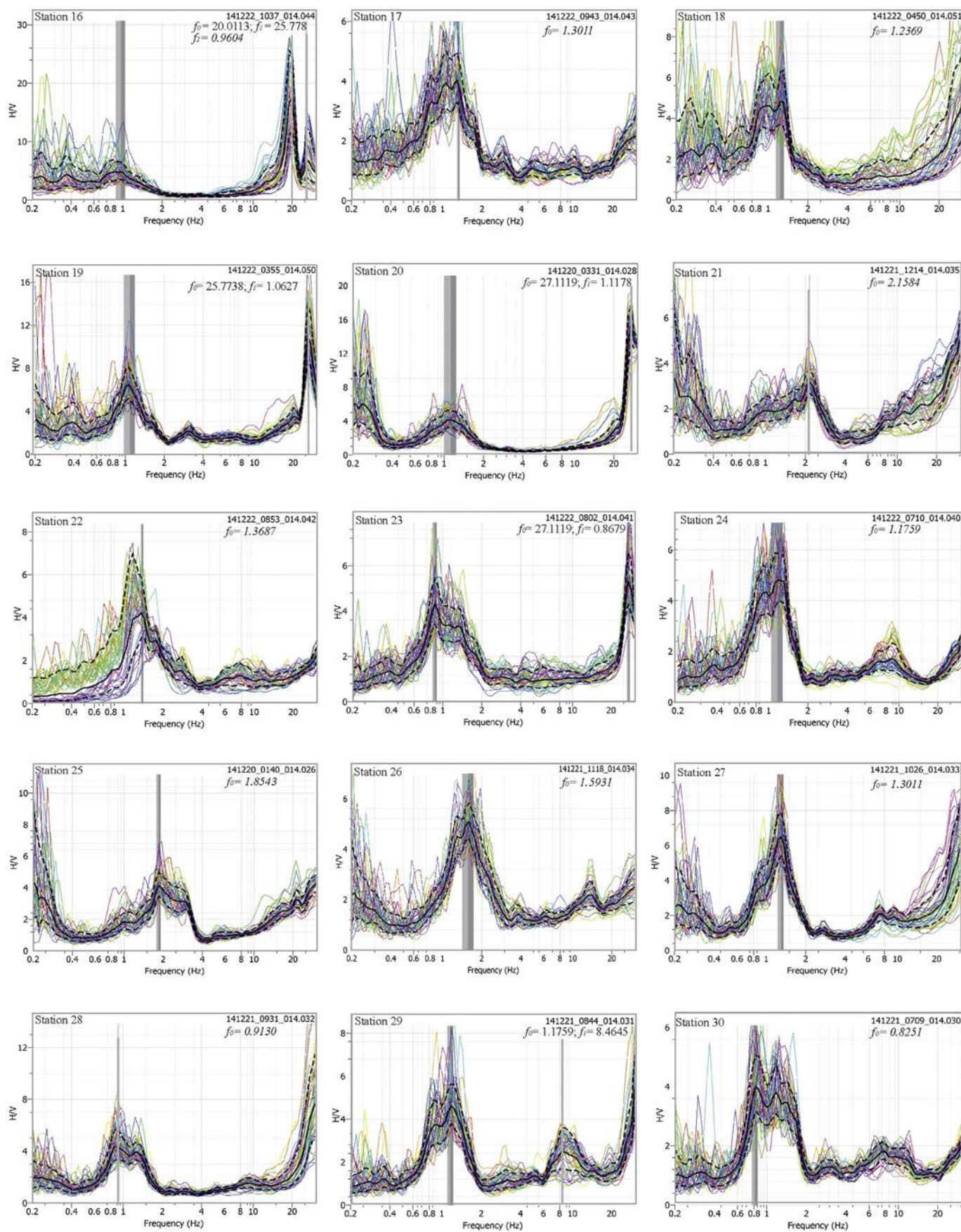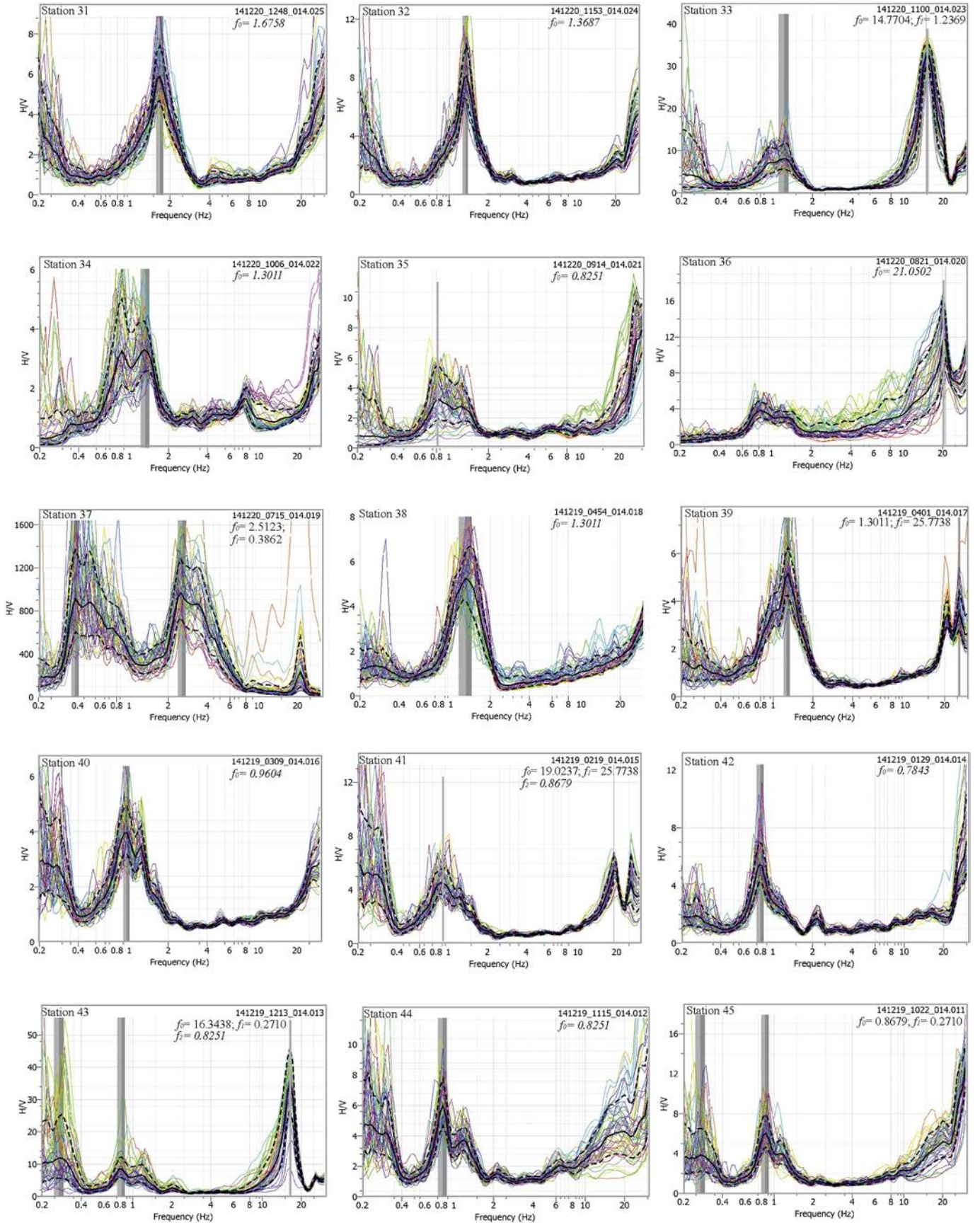
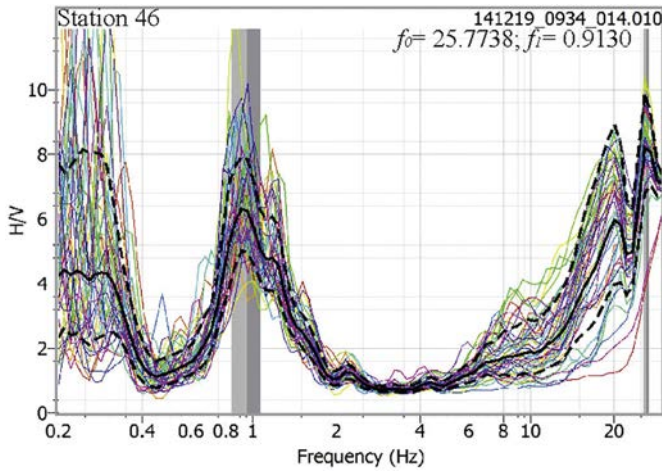**Fig. 3** (*continued*).

Fig. 3 (continued).

Fig. 3 (continued).

3. Microtremor studies and results

Ambient noises persisting in the region act as a source for microtremors. These microtremors generate characteristic frequency which in turn resonates along sediment/rock interfaces having strong acoustic impedance/contrasting density at shallower depth (Ohta et al., 1978; Celebi et al., 1987; Lermo et al., 1988; Field et al., 1990; Hough et al., 1991; Konno and Ohmachi, 1998; Ibs-Von Seht and Wohlenberg, 1999; Aki and Richards, 2002; Parolai et al., 2002). These resonating frequencies derived from microtremors strongly correlate with the velocity of seismic waves and the thickness of the sediments (Ibs-Von Seht and Wohlenberg, 1999; Parolai et al., 2002). Nogoshi and Igarashi (1971) proposed the technique for characterizing amplification of the seismic waves for each site by taking the ratio of the horizontal (NS + EW component) and vertical component (H/V) of the noise spectrum. The H/V ratio normalizes the source effect and enhances site effect. Microtremor method was further enhanced in

reference to their applications (Nakamura, 1989; Field and Jacob, 1993; Delgado et al., 2000; Parolai and Galiana-Merino, 2006; Bonnefoy-Claudet et al., 2006; Garcia-Jerez et al., 2006; Nakamura, 2008; Nakamura, 1989; Boxberger et al., 2011; Mahajan et al., 2011; Bignardi, 2017).

In the present scenario, the microtremor survey was carried out in a grid pattern for upcoming area under Umarsar Lignite Mine lease. Microtremor measurements were taken along forty-six stations at an approximate interval of 250 m (Fig. 1 b and c). The measurements were also carried out at the borehole sites SE of Matanomadh village (Fig. 1a). Lennartz seismometer (5 s period) and a City Shark-II data acquisition system are used in the present survey that records microtremors in NS, EW, and vertical directions for over 40 min, at a rate of 100 samples/s (Sukumaran et al., 2011; Joshi et al., 2018; Sant et al., 2017). Fourier amplitude spectra of H/V components of persisting seismic waves were calculated from forty-six stations using the GEOPSY(SESAME European Project, 2004). The H/V spectral ratios were further plotted between 0.2 Hz and 30 Hz that include the complete range of resonating frequencies recorded within the study area (Fig. 3). Fig. 3 shows the mean value of the frequencies as well as corresponding values of mean ± standard deviation providing error estimates within the resonant frequencies.

Statistically significant H/V spectral peaks were further identified individually using custom-written Matlab code (Joshi et al., 2018; Sant et al., 2017). Peaks are considered to be statistically significant if they are at least one standard deviation greater in amplitude than the baseline activity. These peaks correspond to significant frequencies viz., f_0, f_1, f_2, and f_3,(Table 2 and Fig. 3) which are determined as follows. The frequency corresponding to the largest amplitude peak is taken to be f_0; the frequency corresponding to the next largest peak is taken as f_1 and so on.

The thickness (h) of soil/sediment layer over the bedrock can be related theoretically with the fundamental resonant frequency (f_r) of H/V spectral ratio (Ibs-Von Seht and Wohlenberg, 1999).

$$h = af_r^{\ b} \qquad (1)$$

where a and b are obtained by nonlinear regression between the thickness and the fundamental resonant frequency. For a given
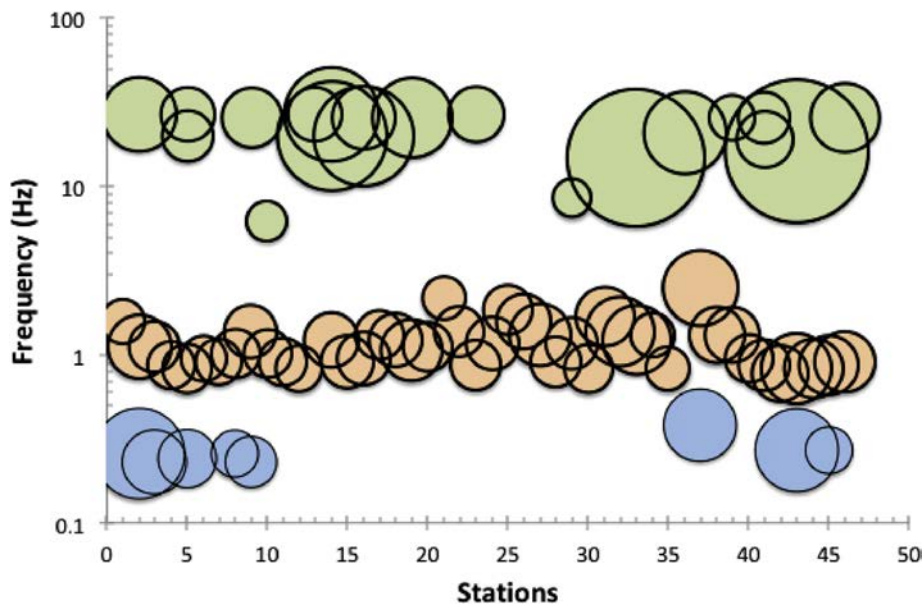

Fig. 4. Bubble diagram shows variation in the resonant frequency of forty-six stations where the diameter of bubbles captures the amplitude of resonant frequency at ≥1 sigma level. The blue colour represent frequency for L_1 interface (M-DT boundary) that ranges between 0.2328 Hz to 0.3862 Hz; orange colour represents frequency for L_2 interface (DT-T boundary) that ranges between 0.7843 Hz to 2.5123 Hz; whereas green colour represents L_3 interface (shale- carbonate hardpans) that ranges from 6.2477 Hz to 27.1119 Hz. (For interpretation of the references to colour in this figure legend, the reader is referred to the web version of this article.)
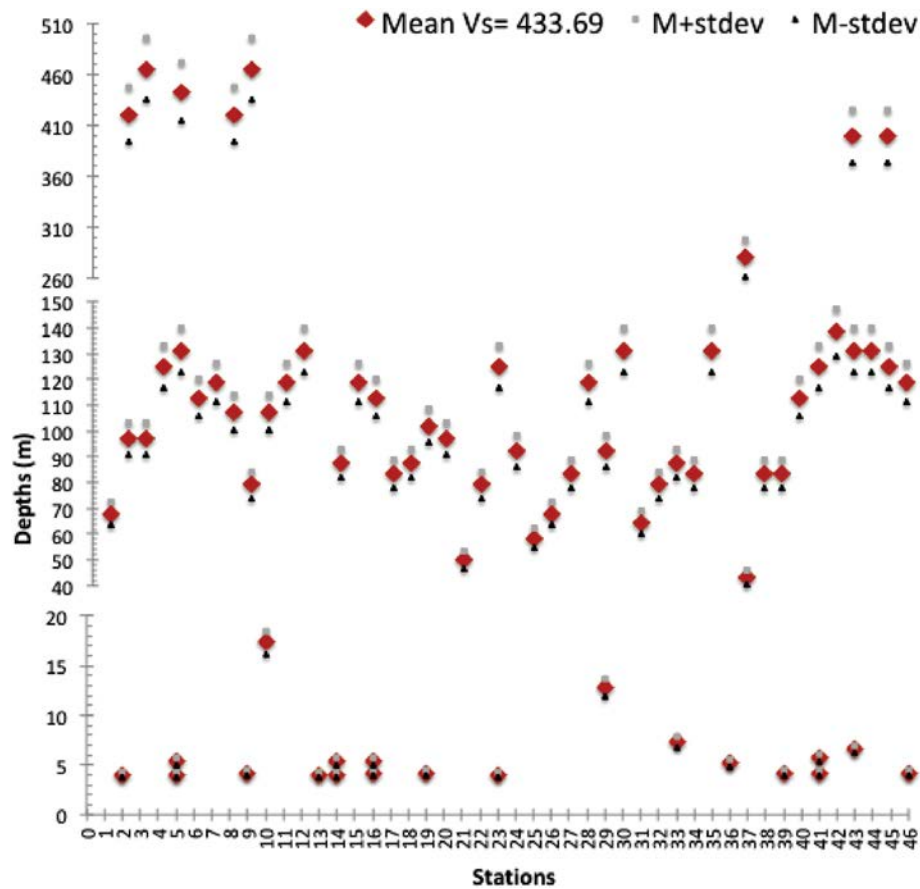
Fig. 5. Scattered plot shows estimation of errors in depth calculation of stations 1 to 46. The depths of interfaces are calculated using velocities derived from three-core sites viz., MMA_Vs (431.6 m/s), MMB_Vs (406.86 m/s) and MMC_Vs (462.6 m/s) using Eq.2. Mean velocity (M_Vs = 433.69 m/s) is used for constructing the model for the study area. The estimate of errors in depths of interfaces is shown by ploting Mean Depth ± standard deviation for each station.

fundamental resonant frequency, if the velocity of seismic waves (V_s) for a given interface is known, the depth of the interface is given by (Parolai et al., 2002):

$$h = V_s/4f_r^2 \qquad (2)$$

Similarly, if the depth of the interface is known based on available core record, the velocity of seismic waves (V_s) can be determined using Eq.(2).

The robust nature of equation in different terrains with single fundamental resonant frequency as well as multiple resonant frequencies is ascertained through work carried out by various workers to sight few examples: Zhao et al. (2007) studied Yinchuan basin, Japan observing the fundamental frequency values are in good agreement with the isopachous line of the Tertiary basement and captures the tectonic variation; Sukumaran et al. (2011) demarcated pre-quaternary morphology in lower Narmada valley, India; Paudyal et al. (2013) worked in Kathmandu Basin estimating thickness of lacustrine sediments suggesting model for basement topography; Benjumea et al. (2016) studied Hontomin, Burgos region in Spain dominated by a shallow complex structure and carbonate rocks suggests H/V technique is a fast and affordable method that enables to obtain a sediment thickness map of a complex near-surface area; Scheib et al. (2016) worked in Nullarbor Plain, Western Australia suggesting passive seismic approach is a useful screening tool for the mineral exploration industry in areas that are under cover allowing for better targeting and cost-reduction;Joshi et al., 2018 distinguished Champaner metasediment from granite pluton inferring role of granite emplacement in deformation of measedimnts; Sant et al., 2017 carried out subsurface mapping of Banni Plains, Kachchh, India inferring structural history; Yan et al., 2018 estimated

thickness of Antarctic ice sheet applying H/V spectrum inversion confirming robust nature of Eq.2.

In the present study, subsurface lithological variation is described based on three exploratory borehole records Core MMA, Core MMB and Core MMC (see section 2, Fig. 1 and Fig. 2). The lithological records along the three cores MMA,MMB and MMC reveals presence of Deccan basalts at depth of 96.53, 86.5 and 93.5 respectively. In the study area, the only substantial interface that would provide a strong impidence contrast is the one along Deccan Trap-Tertiary sedimentary interface. Microtremor measurements at the Core sites MMA,MMB and MMCendorse 1.1178 Hz, 1.1759 Hz and 1.2369 Hz respectively as the most prominent resonaant frequency correlatable with Deccan Trap-Tertiary sedimentary interface.

We calculated velocity (Vs) for the sedimentary unit above the Tertiary sedimentary-Deccan Trap interface for MMA,MMB and MMC stations using Eq.2. We further use mean value of Vs for calculating depth of various other resonanat frequency ensuing from Station 1 to Station 46 in the study area (Table 2). Finally, a terrain base equation is obtain from a scattered plot drawn between resonnant frequency against calculated depth.

$$h = 108.43\, f_r^{-1} \qquad (3)$$

The errors in depth calculation are further estimated taking standard deviation of depths calculated for all 46 stations considering Vs from stations MMA,MMB and MMC. Fig. 4 illustrates calculated mean depth values as well as values of mean depth ± standard deviation.

The resonating frequency for the Umarsar area falls into three distinct groups viz., 0.2328 Hz to 0.3862 Hz (L$_1$ interface: recorded along 8 stations); 0.7843 Hz to 2.5123 Hz (L$_2$ interface: recorded along
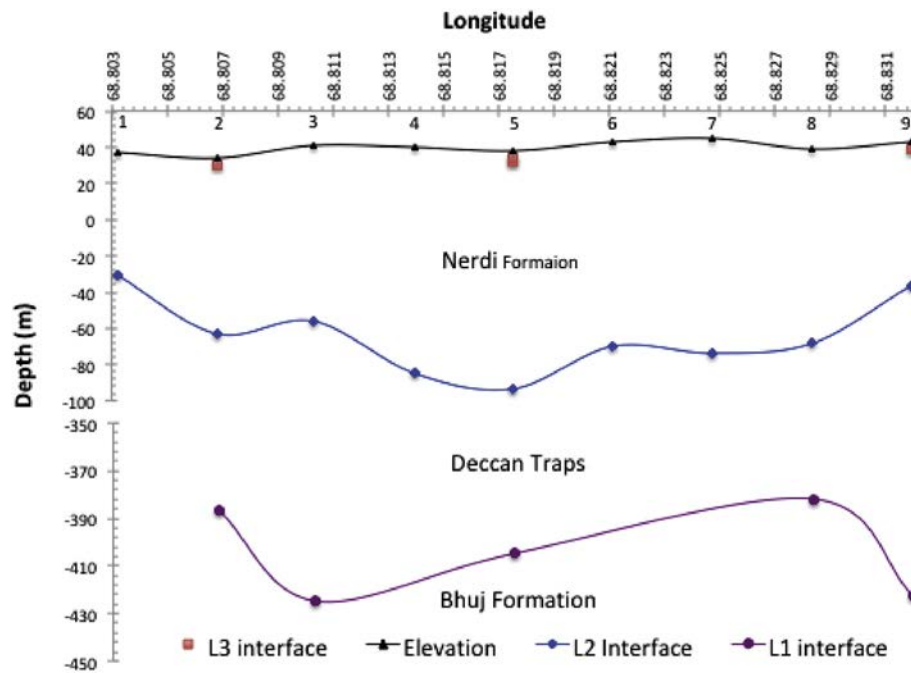
Fig. 6. Cross section across station 1 in west to station 9 in east (Babia syncline) show three layered model viz., M-DT boundary (L_1 interface), DT-Tertiary boundary (L_2 interface) and carbonate hard pans-shale boundary (L_3 interface).

44 stations) and 6.2477 Hz to 27.1119 Hz (L_3 interface: recorded along 20 stations) (Fig. 5).

So as to define L_1, L_2, and L_3 interfaces, we draw a subsurface cross-section from station 1 (in west) to station 9 (in east) (Fig. 6). Based on geology and stratigraphy of Guneri-Mundhan Dome east north east of study area (Biswas, 1977, 2016), Bhuj Formation is likely to extend further west in the study area. The identified interface at depth of 423 m below surface under station 9, interface at depth of 421 m under station 8, is classified as L_1 interface referred as Mesozoic–Deccan Trap boundary (M-DT boundary). The L_2 interface is identified at depth of 131 m (station 5)to 125 m (station 4)from the surface is classified as Deccan Trap -Tertiary sedimentaries (DT-T boundary). Whereas L_3 interface possibly points towards the interfaces between thin intercalated carbonate hard pans within clay of Nerdi Formation at depth of about 4 m to 5.4 m (station 2 and 5). The study further determines thickness of Nerdi formation from 93 m at station 5 to 31 m at station 1)and Deccan Basalt from 368at station 3 to 313 m at station 8.

In the study area, L_1 interface (M-DT boundary) is conspicuous along stations 2, 3, 5, 8, 9, 37, 43, and 45. The depth of M-DT calculated based on Eq.(3) falls within the bracket of about 466 m (station 3 and station 9)to 280 m (station 37) from the surface. The Mesozoic sedimentaries are recorded at the shallower depth around station 37 (280 m), station 43 and station 45 (400 m) whereas deeper depths are recorded along three stations are 9 and 3 (466 m), station 5 (442 m), and station 2 and station 8 (421 m) from the surface (Fig. 7).

L_2 interface is the most pronounced interface recorded along forty-four stations. L_2 Interface demarcates boundary between underlying Deccan Trap and overlaying Tertiary sedimentary. DT-T boundary is observed to be as deep as 138 m (station 42) 131 m (stations 5, 12, 30, 35, 43 and 44) below surface and as shallow as 43 m (station 37) and are exposed along low domal hills further, west of station 1 (Fig. 1). The present studies identify three depressions comprising six depocenters (A B, C, D,E and F)demarcated by two local highs X (demarcating depocenter B—C from D)and Y (demarcating depocenter D from E and F)(Fig. 7).

L_3 interface signifies locally presence of shallow carbonate hardpans of wackestone and packstones that pinch out laterally within shale-clayey Naredi Formation (Fig. 6). Hardpans are encountered at an average depth of 2 m to 3 m, deepest at 11.5 m (station 37).

4. Discussion

The subsurface investigation was carried out applying microtremor H/V spectral ratio technique in upcoming Umarsar lease area western Kachchh. The studies reveal control of pre-Deccan Trap morphology restricting Deccan basalt flow to southwest whereas the pre-Tertiary morphology defines NW-SE trending Babia syncline inscribing local highs and lows that control distribution and thickness of lignite seams within clay-shale sequence and general Naredi Formation (Fig. 7b).

The Mesozoic high (below station 37) forms a subsurface relict of southwestern limb of Guneri-Mundhan dome exposed further NNE of the study area (Fig. 1b). The Guneri-Mundhan dome forms a part of NW-SE, regional trending, arcuate structural grain along Kachchh Mainland hill range viz., Guneri, Mudhan, Jara, Jumara, Nara, Keera, Jhura, Habo, and Khirsar Domes (from west to east: Fig. 1A of Sant et al., 2017) developed because of emplacement of mafic pluton underneath Mesozoic sedimentaries during late Cretaceous (Sen et al., 2016). The Kachchh Mainland Hill range restricts Deccan Trap flows in SW region (Sen et al., 2009). The absence of Deccan basalt flows across Kachchh Mainland hill range (NE) in Banni plains (Sant et al., 2017), Nirona Deep Core and Banni Deep Core (records from DGH) further support role of Mesozoic high in study area. In the present study area the M-DT boundary is encountered as deep as 465 m depth (station 9)and 421 m (stations 2 and station 8)and as shallow as 280 m (station 37).

The depression developed in forefront of Kachchh Mainland hill range in the study area has accumulated Deccan basalt flows. The present study suggests thickness of Deccan basalt (L_1—L_2) ranges between 386 m (station 9)and 208 m (station 37).

The study reveals post-Deccan Trap morphology is decisive for variation in the thickness of lignite bearing sediment sequence (Naredi Formation). The thick shale-clay sequence with lignite seams aggraded over post Deccan Trap morphology within Babia syncline during upper Paleocene- lower Eocene time. The Tertiary floor (DT–T boundary) lies at shallower depth (43 m) at station 37 whereas at deeper levels (138 m) at station 42 and 131 m (stations 5, 12, 30, 43, 44).

Fig. 7 depicts 3D model for the Umarsar lease area that calls to attention three broad pre-Tertiary depression (A-B-C; D and E-F) separated by highs (X and Y). The studies further map six lows (A, B, C, D,E and F)
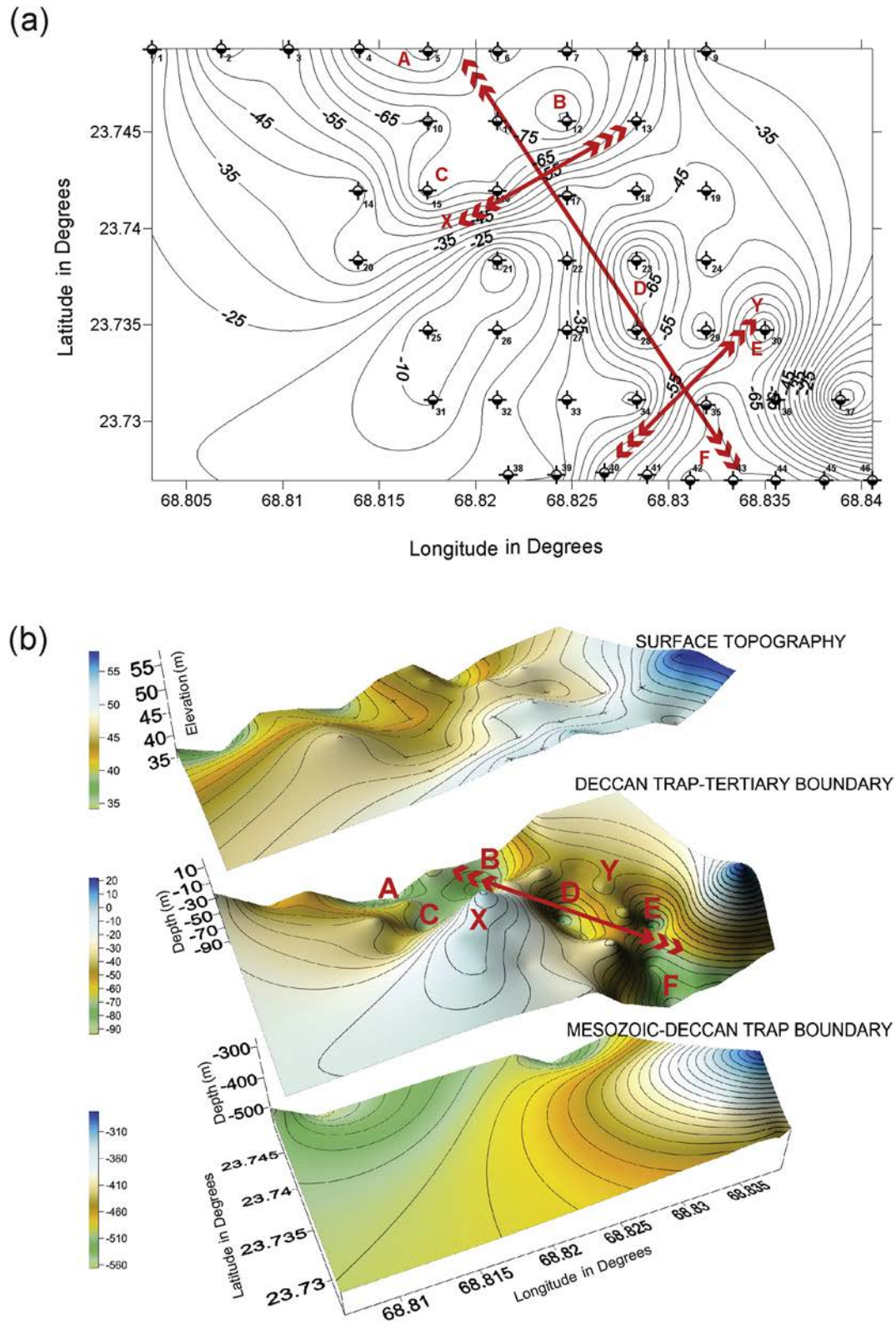
Fig. 7. (a)2D Plan showing palaeo surface morphology of L_2 interface (DT-Tertiary boundary) in upcoming Umarsar lease area. The contours represent highs and lows along DT-T boundary. Microtremor measurement stations and their numbers are shown half filled circle. (b)3D model highlights present day topography of the study area, palaeo surface along L_2 interface (DT-T boundary) and palaeo surface along L_1 interface (M-DT boundary). The palaeo surface modeled at M-DT boundary highlighting Mesozoic high around station 37. Impression of Palaeo topographic high along M-DT boundary is further observed along DT-T boundary and present topography. The palaeo surface modeled at DT-T boundary highlighting NW-SE trending Babia syncline. The model identifies three depressions (A-B-C, D and E-F) separated by two highs (X and Y)that trend NE-SW discordant to the Babia syncline. The study further identifies six Tertiary depocenters (A, B, C, D, E and F)within three depressions and the peripheral margins of the Babia syncline, which are the most potential sites for lignite exploitation.

Table 2

The table displays resonant frequency f_0, f_1, f_2 and f_3 classified based on peak amplification and their respective depth calculated using value of mean velocity M_Vs (433.69 m/s) for forty-six stations in upcoming lease area of Umarsar Lignite Mine.

Station no.	$f0$ (Hz)	M_Vs Depth (m)	$f1$ (Hz)	M_Vs Depth (m)	$f2$ (Hz)	M_Vs Depth (m)	$f3$ (Hz) (Hz)	M_Vs Depth (m)
1	1.5931	68.06						
2	0.2576	420.89	27.1119	4.00	1.1178	97.00		
3	0.2328	465.73	1.1178	97.00				
4	0.8679	124.93						
5	0.2449	442.72	27.1119	4.00	20.0113	5.42	0.8251	131.41
6	0.9604	112.89						
7	0.913	118.75						
8	1.0102	107.33	0.2576	420.89				
9	25.7738	4.21	1.3687	79.22	0.2328	465.73		
10	1.0102	107.33	6.2477	17.35				
11	0.913	118.75						
12	0.8251	131.41						
13	27.1119	4.00						
14	20.0113	5.42	1.2369	87.66	27.1119	4.00		
15	0.913	118.75						
16	20.0113	5.42	25.7738	4.21	0.9604	112.89		
17	1.3011	83.33						
18	1.2369	87.66						
19	25.7738	4.21	1.0627	102.03				
20	1.1178	97.00						
21	2.1584	50.23						
22	1.3687	79.22						
23	27.1119	4.00	0.8679	124.93				
24	1.1759	92.20						
25	1.8543	58.47						
26	1.5931	68.06						
27	1.3011	83.33						
28	0.913	118.75						
29	1.1759	92.20	8.4645	12.81				
30	0.8251	131.41						
31	1.6758	64.70						
32	1.3687	79.22						
33	14.7704	7.34	1.2369	87.66				
34	1.3011	83.33						
35	0.8251	131.41						
36	21.0502	5.15						
37	2.5123	43.16	0.3862	280.74				
38	1.3011	83.33						
39	1.3011	83.33	25.7738	4.21				
40	0.9604	112.89						
41	19.0237	5.70	25.7738	4.21	0.8679	124.93		
42	0.7843	138.24						
43	16.3438	6.63	0.271	400.08	0.8251	131.41		
44	0.8251	131.41						
45	0.8679	124.93	0.271	400.08				
46	25.7738	4.21	0.913	118.75				

within three depression and shallow peripheral regions that has significant potential in encountering thick lignite seams. The maximum thickness estimated for Tertiary Formation along these lows are A(131 m), B(131 m), C(102 m), D(79 m) E(131 m) and F(131 m). Decrease in the sediment thickness along X(87 m to 83 m) and Y(83 m to 92 m) suggest X and Y are pre-Tertiary highs. The study proposes that variable thickness in Tertiary sequence is due to uneven pre-Tertiary topography.

The microtremor measurement is the most economical technique for estimating thickness of lignite bearing sedimentary sequence, Deccan Traps and depth of Mesozoic sedimentary rocks. The records generated further help to build subsurface morphological models for prominent interfaces (M-DT boundary and DT-T boundary). The present research is a step forward towards economical assessment of mining lease areas through controlled drill hole plan and for estimation of reserves.

5. Conclusions

1. The present article discusses microtremor H/V spectral ratio technique as a rapid and economical tool to assess mining lease areas and develop controlled drill hole plan and estimate reserves.

2. The microtremor H/V spectral ratio technique identifies highs, lows and peripheral areas providing overall geometry of NW-SE trending lignite bearing Tertiary basin (Babia Syncline)

3. The microtremor H/V spectral ratio technique successfully deciphers rheological interphases. Viz., Mesozoic– Deccan Trap boundary (L_1 interface: 0.2328 Hz to 0.3862 Hz), Deccan Trap- Tertiary boundary (L_2 interface: 0.7843 Hz to 2.5123 Hz) and boundaries between shale- carbonate hardpans within sediment sequence belonging to Naredi Formation (L_3 interface: 6.2477 Hz to 27.1119 Hz).

4. Pre Deccan Trap image of Umarsar lease area distinguishes Mesozoic high (below station 37) which forms a subsurface relict of southwestern limb of Guneri-Mundhan dome exposed further NNE of the study area. The dome forms part of NW-SE regional arcuate structure (Kachchh Mainland Hill range) that restricts Deccan Trap flows towards SW.

5. The present study estimates Mesozoic–Deccan Trap boundary at depth of 465 m depth (station 9)and 421 m (stations 2 and station 8)and as shallow as 280 m (station 37) whereas thickness of Deccan basalt (L_1-L_2) is estimated between 386 m (station 9)and 237 m (station 37).

6. Pre Tertiary image of the Umarsar lease area highlights three broad pre-Tertiary depression (A-B-C; D and E-F) separated by highs

(Xand Y). The thickness of lignite bearing Tertiary deposits is estimated from 138 m to 43 m. The studies further map six lows (A, B, C, D,E and F)within three depressions and enhances shallow peripheral regions that have proved to encounter thick lignite seams.

Acknowledgement

References

Agrawal, G.C., 1984. Further Studies on Tertiary and Quaternary Sequences of South Gujarat with Reference to their Structural Style and Geomorphic Expressions. PhD Thesis. Maharaja Sayajirao University of Baroda, p. 177 (unpublished).

Aki, K., Richards, P.G., 2002. Quantitative Seismology. second ed. University Science Book, p. 687.

Benjumea, B., Macau, A., Gabàs, A., Figueras, S., 2016. Characterization of a complex near-surface structure using well logging and passive seismic measurements. Solid Earth 7, 685–701.

Bignardi, S., 2017. The uncertainty of estimating the thickness of soft sediments with the HVSR method: a computational point of view on weak lateral variations. J. Appl. Geophys. 145, 28–38.

Biswas, S.K., 1977. Mesozoic stratigraphy of Kutch, Gujarat. Quart. Jour. Geol. Min. Met. Soc. Ind. 43, 223–236.

Biswas, S.K., 1992. Tertiary stratigraphy of Kutch. J. Palaeontol. Soc. India 37, 1–29.

Biswas, S.K., 2016. Mesozoic and Tertiary stratigraphy of Kutch (Kachchh) – a review. Geol. Soc. India Spec. Publ. 6, 1–24.

Bonnefoy-Claudet, S., Cornou, C., Bard, P.Y., Cotton, F., Moczo, P., Kristek, J., Fäh, D., 2006. H/V ratio: a tool for site effects evaluation. Results from 1-D noise simulations. Geophys. J. Int. 167, 827–837.

Boxberger, T., Picozzi, M., Parolai, S., 2011. Shallow geology characterization using Rayleigh and love wave dispersion curves derived from seismic noise array measurements. J. Appl. Geophys. 75 (2), 345–354.

Celebi, M., Dietel, C., Prince, J., Onate, M., Chavez, G., 1987. Site amplification in Mexico City (determined from 19 September 1985 strong-motion records and from recording of weak motions). Ground Mot. Eng. Seismol. 141–152.

Chandra, P.K., Chowdhary, L.R., 1969. Stratigraphy of the Cambay Basin. Bull. ONGC 6, 37–50.

Das, S., Singh, H., Tiwari, D., Parulkar, S.N., 2006. Reservoir Classification and Geological Remodeling of Kalol Sands of Sobhasan Complex, North Cambay Basin, India. Geohorizons. 11 pp. 1–9.

Delgado, J., Lopez Casado, C., Estevez, A.C., Giner, J., Cuenca, A., Molina, S., 2000. Mapping soft soils in the Segura river valley (SE Spain): a case study of microtremors as an exploration tool. J. Appl. Geophys. 45, 19–32.

Dutta, S., Mathews, Runcie P., Singh, B.D., Tripathi, S.M., Singh, A., Saraswati, P.K., Banerjee, S., Mann, U., 2011. Petrology, palynology and organic geochemistry of Eocene lignite of Matanomadh, Kutch Basin, western India: Implications to depositional environment and hydrocarbon source potential. Int. J. Coal Geol. 85 (2011), 91–102.

Field, E., Jacob, K., 1993. The theoretical response of sedimentary layers to ambient seismic noise. Geophys. Res. Lett. 20, 2925–2928.

Field, E.H., Hough, S.E., Jacob, K.H., 1990. Using microtremors to assess potential earthquake site response: a case study in Flushing Meadows, New York City. Bull. Seismol. Soc. Am. 80, 1456–1480.

Garcia-Jerez, A., Luzon, F., Navarro, M., Perez-Ruiz, J.A., 2006. Characterization of the sedimentary cover of the Zafarraya basin, southern Spain, by means of ambient noise. Bull. Seismol. Soc. Am. 96, 957–967.

Hough, S.E., Field, E.H., Jacob, K.H., 1991. Using Microtremors to Assess Site-Specific Earthquake Hazard. Earthquake Engineering Research Institute, p. 385.

Ibs-Von Seht, M., Wohlenberg, J., 1999. Microtremor measurements used to map thickness of soft sediments. Bull. Seismol. Soc. Am. 89, 250–259.

Indian Minerals Yearbook 2015 Coal & Lignite Part- III: Mineral Reviews, 2017. Published by Indian Bureau of Mines, Ministry of Mines, Government of India. Edition. 54, pp. 1–24 (www.ibm.gov.in).

Joshi, A.U., Sant, D.A., Parvez, I.A., Rangarajan, G., Limaye, M.A., Mukherjee, S., Charola, M.J., Bhatt, M.N., Mistry, S.P., 2018. Sub-surface profiling of granite pluton using microtremor method: southern Aravalli, Gujarat, India. Int. J. Earth Sci. 107, 191–201.

Khozyem, H., Adatte, T., Keller, G., Spangenberg, Saravanan, N., Bajpai, S., 2013. Paleoclimate and paleoenvironment of the Naredi formation (early eocene), Kutch, Gujarat, India. Geol. Soc. India Spec. Publ. 1, 165–182. https://doi.org/10.1007/s00531-017-1482-9 2013.

Konno, K., Ohmachi, T., 1998. Ground-motion characteristics estimated from spectral ratio between horizontal and vertical components of microtremor. Bull. Seismol. Soc. Am. 88, 228–241.

Kumar, Rajak Pramod, Singh, Vijay Kumar, Kumar, Dharmendra, 2014. Lignite resources of Bikaner and their utilization. Energy Technologies, Climate Change and Environmental Sustainability: Innovative Perspective ISBN: 978-93-83083-87-9, pp. 62–68.

Lermo, J., Rodriguez, M., Singh, S.K., 1988. The Mexico earthquake of September 19, 1985 natural period of sites in the valley of Mexico from microtremor measurements and strong motion data. Earthquake Spectra 4, 805–814.

Mahajan, A.K., Galiana-Merino, J.J., Lindholm, C., Arora, B.R., Mundepi, A.K., Rai, N., Chauhan, N., 2011. Characterization of the sedimentary cover at the Himalayan foothills using active and passive seismic techniques. J. Appl. Geophys. 73 (3), 196–206.

Nakamura, Y., 1989. A method for dynamic characteristics estimation of subsurface using microtremor on the ground surface. Quart. Rep. Railway Tech. Res. Inst. 30, 25–33.

Nakamura, Y., 2008. On the H/V spectrum. The 14th World Conference on Earthquake Engineering, October 12–17, 2008, Beijing, China, pp. 1–10.

Nogoshi, M., Igarashi, T., 1971. On the amplitude characteristics of microtremor (part 2). J. Seismol. Soc. Jpn. 24, 26–40.

Ohta, Y., Kagami, H., Goto, N., Kudo, K.A., 1978. Observation of 1- to 5-secondmicrotremors and their application to earthquake engineering. Part I: comparison with long-period accelerations at the Tokachi-oki earthquake of 1968. Bull. Seismol. Soc. Am. 68, 767–779.

Parolai, S., Galiana-Merino, J.J., 2006. Effect of transient seismic noise on estimates of h/v spectral ratios. Bull. Seismol. Soc. Am. 96, 228–236.

Parolai, S., Bormann, P., Milkereit, C., 2002. New relationships between Vs, thickness of sediments, and resonance frequency calculated by the H/V ratio of seismic noise for the Cologne area (Germany). Bull. Seismol. Soc. Am. 92, 2521–2527.

Paudyal, Y.R., Yatabe, R., Bhandary, N.P., et al., 2013. Basement topography of the Kathmandu basin using microtremor observation. J. Asian Earth Sci. 62, 627–637.

Sahni, A., Saraswati, P.K., Rana, R.S., Kumar, K., Singh, H., Alimohammadin, H., Sahni, A., Rose, K.D., Singh, L., Smith, T., 2006. Temporal constraints and depositional palaeoenvironments of the Vastan Lignite Sequence, Gujarat: Analogy for the Cambay shale hydrocarbon source rock. Indian J. Petrol. Geol. 15, 1–20.

Sanfilipo, J.R., Christopher, W., Mohammad, F., Mujeeb, A., Khan, S.A., Mehtab-Ur-Rahman, Chandio A.H., Khan, R.A., 1992. Potential for the Occurrence of Thick Lignite Deposits in the Thar Desert and Adjacent Lower Indus Plain, Sindh Province, PakistanOpen-File Report 92-576. (Report prepared jointly by the Geological Survey of Pakistan and the U.S. Geological Survey under the auspices of the U.S. Agency for International Development). pp. 1–31.

Sant, D.A., Parvez, I.A., Rangarajan, G., Patel, S.J., Bhatt, M.N., Sanoop, S.T.A., 2017. Profiling along Banni Plains and Bounding Faults, Kachchh, Western India using Microtremors Method. J. Asian Earth Sci. 146, 326–336.

Saraswati, P.K., Banerjee, S., Urbashi Sarkar, U., Chakraborty, S., Khanolkar, S., 2016. Eocene Depositional Sequence and Cycles in Kutch Special Publication Geological Society of India No.6, 2016. pp. 46–56.

Scheib, A., Morris, P., Murdie, R., Delle Piane, C., 2016. A passive seismic approach to estimating the thickness of sedimentary cover on the Nullarbor Plain, Western Australia. Aust. J. Earth Sci. 63 (5), 583–598.

Sen, G., Bizimis, M., Das, R., Paul, D.K., Ray, A., Biswas, S., 2009. Deccan plume, litho- sphere rifting, and volcanism in Kutch, India. Earth Planet. Sci. Lett. 277, 101–111.

Sen, G., Hames, W.E., Paul, D.K., Biswas, S.K., Ray, A., Sen, I.S., 2016. Pre-Deccan and Deccan magmatism in Kutch, India: implications of new 40Ar/39Ar ages of intrusions. Spec. Publ. J. Geol. Soc. India 6, 211–222.

SESAME European Project EVG1-CT-2000–00026, 2004. GEOPSY Software – Download Site < http://www.geopsy.org >.

Sukumaran, P., Parvez, I.A., Sant, D.A., Rangarajan, G., Krishnan, K., 2011. Profiling of late Tertiary–early Quaternary surface in the lower reaches of Narmada valley using microtremors. J. Asian Earth Sci. 41, 325–334.

Thakur, O.P., Alpana, Singh, Singh, B.D., 2010. Petrographic characterization of Khadsaliya lignites, Bhavnagar district, Gujarat. Geol. Soc. India 76, 40–46 July 2010.

World Energy Council, 2013. World Energy Resources: Coal. pp. 1–13 (https://www.worldenergy.org/wp-content/uploads/2013/10/WER_2013_1_Coal.pdf).

Yan, P., Li, Z., Fei Li, F., Yang, Y., Hao, W., Feng Bao, F., 2018. Antarctic ice sheet thickness estimation using the H/V spectral ratio method with single station seismic ambient noise. The Cryosphere Discussions. 12, pp. 795–810.

Zhao, B., Xie, X., Chai, C., Ma, H., Xu, X., Peng, D., Yin, W., Tao, J., 2007. Imaging the graben structure in the deep basin with a microtremor profile crossing the Yinchuan City. J. Geophys. Eng. 4, 293–300.